

Reaction Rate Theory for Electric Field Catalysis in Solution

Sohang Kundu¹ and Timothy C. Berkelbach^{1,2, a)}

¹⁾*Department of Chemistry, Columbia University, New York, New York 10027, USA*

²⁾*Initiative for Computational Catalysis, Flatiron Institute, New York, New York 10010, USA*

The application of an external, oriented electric field has emerged as an attractive technique for manipulating chemical reactions. Because most applications occur in solution, a theory of electric field catalysis requires treatment of the solvent, whose interaction with both the external field and the reacting species modifies the reaction energetics and thus the reaction rate. Here, we formulate such a transition state theory using a dielectric continuum model, and we incorporate dynamical effects due to solvent motion via Grote-Hynes corrections. We apply our theory to the Menshutkin reaction between CH_3I and pyridine, which is catalyzed by polar solvents, and to the symmetric $\text{S}_{\text{N}}2$ reaction of F^- with CH_3F , which is inhibited by polar solvents. At low applied field strengths when the solvent responds linearly, our theory predicts near-complete quenching of electric field catalysis. However, a qualitative treatment of the nonlinear response (i.e., dielectric saturation) shows that catalysis can be recovered at appreciable field strengths as solvent molecules begin to align with the applied field direction. The Grote-Hynes correction to the rate constant is seen to vary nonmonotonically with increasing solvent polarity due to contrasting effects of the screening ability, and the longitudinal relaxation time of the solvent.

I. INTRODUCTION

The impact of oriented electric fields on chemical reactions has been increasingly studied in recent years, especially in the context of selectivity and catalysis; for an overview, we refer to recent review articles and perspectives.¹⁻⁵ The application of an oriented, external electric field to control a chemical reaction has been clearly demonstrated using a scanning tunneling microscope break junction,^{6,7} but this method is hard to scale to industrial levels. Alternatively, chemical reactions have been influenced using the electric field formed spontaneously at the interface of an electrode and an electrolyte^{8,9} and the electric field due to functional groups installed on molecular catalysts.^{10,11}

Significant computational work has been done in this field using gas phase quantum chemistry,¹²⁻¹⁸ in conjunction with hybrid quantum mechanics/molecular mechanics¹⁹⁻²¹ as well as classical^{22,23} and ab initio²⁴⁻²⁶ molecular dynamics simulations. This has led to important qualitative understanding of the interaction between a molecule's electronic structure and an external electric field. However, there has been considerably less work on the role of solvents and their dynamics, which is an important topic given that scalable methods of electric field catalysis will likely occur in solution.

Consider a molecular system undergoing a chemical reaction from reactant (R) to transition state (TS) to product (P). Assuming a one-dimensional reaction coordinate, the transition state theory (TST) approximation²⁷ to the rate constant for barrier crossing is

$$k_0 = \frac{\omega_{\text{R}}}{2\pi} e^{-\beta\Delta V^\ddagger} \quad (1)$$

where $\Delta V^\ddagger = V_{\text{TS}} - V_{\text{R}}$ is the barrier height, ω_{R} is the vibrational frequency in the reactant well, and $\beta = 1/k_{\text{B}}T$. In the presence of an external electric field \mathbf{E}_{ext} , the energy of the

molecular system is changed, to lowest order, by $-\boldsymbol{\mu} \cdot \mathbf{E}_{\text{ext}}$ (throughout this work, we neglect the molecular polarizability).

The barrier height is modified,

$$\Delta V^\ddagger(\mathbf{E}_{\text{ext}}) = \Delta V^\ddagger - \Delta\boldsymbol{\mu}^\ddagger \cdot \mathbf{E}_{\text{ext}} \quad (2)$$

where $\Delta\boldsymbol{\mu}^\ddagger = \boldsymbol{\mu}_{\text{TS}} - \boldsymbol{\mu}_{\text{R}}$ is the dipole moment difference between the transition state and the reactant configuration. The catalytic effect of the external field is then given by the ratio

$$k(\mathbf{E}_{\text{ext}})/k(0) = \exp\left(\beta\Delta\boldsymbol{\mu}^\ddagger \cdot \mathbf{E}_{\text{ext}}\right), \quad (3)$$

where the zero-field rate constant is $k(0) = k_0$ in Eq. (1). How large is the above effect? For a dipole moment difference of $|\Delta\boldsymbol{\mu}^\ddagger| = 10$ D and an electric field of strength $|\mathbf{E}| = 1$ V/nm, the energy change is about 5 kcal/mol. Recalling that $k_{\text{B}}T \approx 0.6$ kcal/mol at 300 K, the change to the rate is a factor of about 4×10^3 , and the rate can be increased or decreased depending on the relative orientations of the electric field and the dipole moment difference. For higher values of $|\Delta\boldsymbol{\mu}^\ddagger|$, the effect is even more pronounced.

For reactions occurring in solution, a polar solvent interacts with both the electric field and the molecular system, modifying the thermodynamics and kinetics of the chemical reaction. Therefore, this simple picture of electric field catalysis must be modified, which is the aim of the present work. First, we develop a microscopic electrostatic theory to define free energies for use within adiabatic TST.

Second, we consider the dynamical response of the solvent and calculate dynamical corrections to the rate constant within Grote-Hynes theory.²⁸ We apply our theory to two $\text{S}_{\text{N}}2$ -like reactions, the Menshutkin reaction of pyridine with CH_3I and a symmetric $\text{S}_{\text{N}}2$ reaction of F^- with CH_3F .

^{a)}Electronic mail: t.berkelbach@columbia.edu

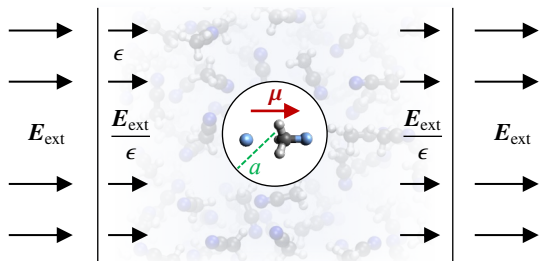


FIG. 1. Dielectric arrangement used in this work to model the electrodynamics of a molecular complex with dipole moment μ in a spherical cavity of radius a in a polar solvent with dielectric constant ϵ in an externally applied electric field \mathbf{E}_{ext} .

II. RESULTS AND DISCUSSION

A. Adiabatic Transition State Theory

To study the influence of a polar solvent, we use the setup shown in Fig. 1. The molecule is modeled as a dipole μ in a spherical cavity of radius a . The dipole polarizes the surrounding dielectric, which induces a constant reaction field²⁹ inside the cavity,

$$\mathbf{E}_{\text{rxn}} = \frac{2}{a^3} \frac{\epsilon - 1}{2\epsilon + 1} \mu \quad (4)$$

where ϵ is the dielectric constant of the solvent (here and throughout we use atomic units, for which $4\pi\epsilon_0 = 1$). Simultaneously, an external field \mathbf{E}_{ext} is applied to the dielectric, inside of which the field is reduced in magnitude to $\mathbf{E}_{\text{ext}}/\epsilon$.

We emphasize that throughout this work, \mathbf{E}_{ext} is the electric field that would exist in the absence of a solvent. Due to the formation of bound charges on the surface of the spherical cavity, the external electric field generates an electric field inside the cavity,

$$\mathbf{E}_{\text{in}} = \frac{3\epsilon}{2\epsilon + 1} \frac{\mathbf{E}_{\text{ext}}}{\epsilon} = \frac{3}{2\epsilon + 1} \mathbf{E}_{\text{ext}}. \quad (5)$$

By the linearity of the Poisson equation, the total field in the cavity is the sum,

$$\mathbf{E}_{\text{tot}} = \mathbf{E}_{\text{rxn}} + \mathbf{E}_{\text{in}}, \quad (6)$$

leading to the interaction free energy

$$G = -\mu \cdot \mathbf{E}_{\text{tot}} = -\frac{2\mu^2}{a^3} \frac{\epsilon - 1}{2\epsilon + 1} - \frac{3}{2\epsilon + 1} \mu \cdot \mathbf{E}_{\text{ext}}. \quad (7)$$

Note that the solvation energy, arising from the interaction with the reaction field, is always stabilizing, whereas the interaction with the external field depends on orientation.

The TST rate constant in solution is thus

$$k_{\text{TST}}(\mathbf{E}_{\text{ext}}) = \frac{\omega_{\text{R}}}{2\pi} e^{-\beta\Delta G^\ddagger(\mathbf{E}_{\text{ext}})} \quad (8)$$

where

$$\Delta G^\ddagger(\mathbf{E}_{\text{ext}}) = \Delta V^\ddagger - \frac{2(\mu_{\text{TS}}^2 - \mu_{\text{R}}^2)}{a^3} \frac{\epsilon - 1}{2\epsilon + 1} - \frac{3}{2\epsilon + 1} \Delta\mu^\ddagger \cdot \mathbf{E}_{\text{ext}}. \quad (9)$$

Whether the solvation effect is catalytic depends on the sign of $\mu_{\text{TS}}^2 - \mu_{\text{R}}^2$, which is a well-known effect for chemical reactions in polar solvents. Clearly, in a nonpolar solvent with $\epsilon = 1$, this rate constant reduces to Eq. (3).

The theory so far treats the solvent as a linear dielectric, i.e., in the absence of the cavity, the solvent polarization is $\mathbf{P} = (\epsilon - 1)\mathbf{E}_{\text{ext}}$. In this approximation, the effect of the reaction field and the external field are separable, and the catalytic effect of the external field compared to the reaction in solution is simply determined by the ratio

$$k_{\text{TST}}(\mathbf{E}_{\text{ext}})/k_{\text{TST}}(0) = \exp\left[3\beta\Delta\mu^\ddagger \cdot \mathbf{E}_{\text{ext}}/(2\epsilon + 1)\right]. \quad (10)$$

Comparison with Eq. (3) shows that the effect of a polar solvent is merely to screen the electric field, reducing its strength by about a factor of ϵ . For common polar solvents with $\epsilon \gtrsim 10$, this would severely limit the applicability of electric field catalysis in solution.

However, real solvents behave as nonlinear dielectrics, and when they are subjected to large electric fields, the polarization saturates with increasing field strength due to the near-complete alignment of molecular dipole moments. This phenomenon, known as dielectric saturation, can be approximately modeled by using a dielectric constant that depends on the strength of the applied electric field, leading to a polarization $\mathbf{P} = [\epsilon(E_{\text{ext}}) - 1]\mathbf{E}_{\text{ext}}$. A common approximation is Booth's equation,³⁰

$$\epsilon(E) = 1 + \frac{3E_c}{E} (\epsilon - 1) L\left(\frac{E}{E_c}\right), \quad (11)$$

where ϵ is the field-free dielectric constant, $L(x) = \coth(x) - 1/x$ is the Langevin function, and

E_c is a microscopic field parameter characteristic of the solvent.

Within this model, the dielectric constant decreases with increasing field strength and saturates to $\epsilon = 1$ when $E \gg E_c$. Using this field-dependent dielectric constant in Eq. (10) yields

$$k_{\text{TST}}(\mathbf{E}_{\text{ext}})/k_{\text{TST}}(0) = \exp\left[\frac{3\beta\Delta\mu^\ddagger \cdot \mathbf{E}_{\text{ext}}}{2\epsilon(E_{\text{ext}}) + 1}\right] \times \exp\left[\frac{2\beta(\mu_{\text{TS}}^2 - \mu_{\text{R}}^2)}{a^3} \left(\frac{\epsilon(E_{\text{ext}}) - 1}{2\epsilon(E_{\text{ext}}) + 1} - \frac{\epsilon - 1}{2\epsilon + 1}\right)\right], \quad (12)$$

which is one of the main results of this work.

The first system to which we apply this theory is the Menschutkin reaction of pyridine with CH_3I , which was studied in the same context of electric field catalysis a few years ago by Shaik and co-workers²³ using a combination of atomistic molecular dynamics (MD) simulations and quantum chemistry calculations with implicit and explicit solvent. In the absence of an external electric field, the solvent alone was found to have a catalyzing effect on the reaction (in acetonitrile, the barrier is lowered by 8.5 kcal/mol), which is a well-known effect^{31,32}

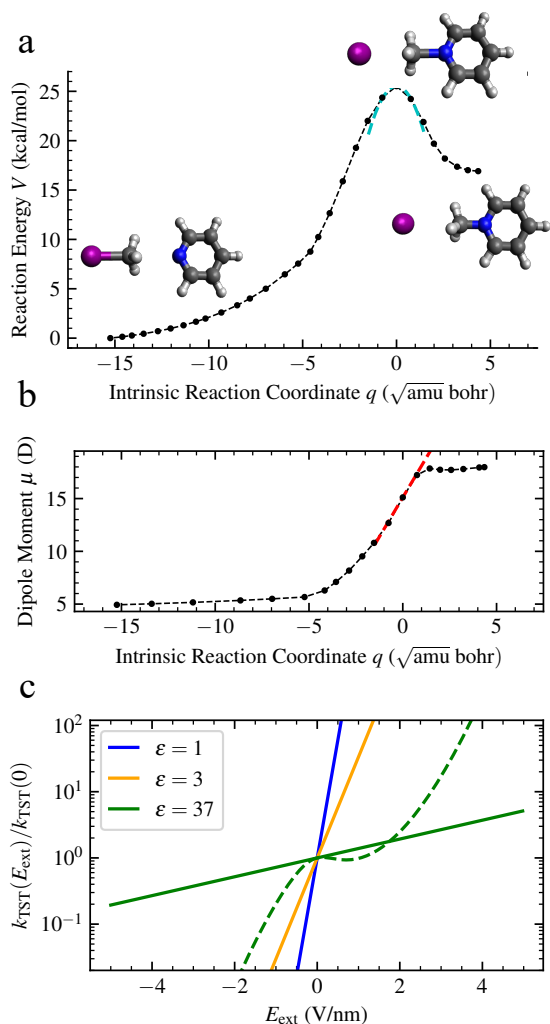


FIG. 2. (a) Reaction energy and (b) dipole moment along the mass-weighted intrinsic reaction coordinate of the Menshutkin reaction between CH_3I and pyridine. The cyan dashed line in (a) highlights the curvature of the reaction energy at the TS, and the red dashed line in (b) indicates the slope of the dipole moment at the TS. (c) The adiabatic TST rate enhancement due to an external electric field in various solvents with the dielectric constants indicated ($\epsilon = 37$ corresponds to acetonitrile). The dashed green line incorporates nonlinear effects of dielectric saturation for acetonitrile.

from previous experimental and computational studies. Under an applied electric field, polarization of the solvent was found to create a near-complete screening effect, and only when the solvent was maximally polarized beyond a certain external field strength (about 1.5 V/nm in acetonitrile), the catalytic effect was recovered, leading to an additional reduction of the barrier height by 10.6 kcal/mol at $E = 5$ V/nm. We will use these results as a test of our theory, and the numerical comparisons are summarized in Tab. I.

Using the ORCA package,³³ we calculated the minimum energy pathway and dipole moment for the intrinsic reaction coordinate^{34,35} (IRC), as shown in Fig. 2a and Fig. 2b respectively. Calculations were performed using unrestricted density

functional theory (DFT) with the B3LYP functional^{36,37} and the def2-TZVP basis set^{38,39} (additional details are given in the Supporting Information), leading to a barrier height of $\Delta V^\ddagger = 25.5$ kcal/mol. In the gas phase, this reaction proceeds from neutral reactants to ionic products, such that the dipole moment is increasing in magnitude throughout the reaction. We find $\mu_R = 4.9$ D and $\mu_{\text{TS}} = 15.1$ D, such that

$\mu_{\text{TS}}^2 - \mu_R^2 > 0$, confirming that the reaction is catalyzed by a polar solvent. Based on solvent distribution functions calculated in another recent MD study,⁴⁰ we estimate a cavity radius of $a = 0.7$ nm.

Using these parameters, we find that, when no field is applied, the barrier height is lowered by 8.2 kcal/mol in acetonitrile solvent ($\epsilon = 37$). This is in remarkably good agreement with the value of 8.5 kcal/mol found by atomistic simulations,²³ indicating an accurate parameterization of our model.

In Fig. 2c, we plot the rate enhancement obtained due to an external electric field from Eq. (10), without dielectric saturation. We consider three values of the solvent dielectric constant, $\epsilon = 1, 3$, and 37. As expected, the logarithm of the enhancement is linearly proportional to the field, with a slope proportional to $(\epsilon + 1)^{-1}$. For large external fields and weakly polar solvents, the rate modification can be as much as 10^5 . However, due to the screening effect of polar solvents, the modification is small: for acetonitrile, with $\epsilon = 37$, even an external field of 5 V/nm modifies the rate by only a factor of 5.

In the same figure, we also plot the rate enhancement in acetonitrile including dielectric saturation, i.e., using Eq. (12). Following Ref. 41, we parameterize the Booth model with $E_c = 0.15$ V/nm for acetonitrile. We see that the rate behavior is more complicated, and importantly shows a stronger catalytic effect at large fields, in agreement with the simulations of Shaik and co-workers.²³ Interestingly, the change in rate for a saturating dielectric is no longer monotonic and is asymmetric with respect to the direction of the applied field.

To understand this change in behavior, let us focus on the contributions of the reaction field and the external field separately. Saturation reduces the ability of the solvent to solvate the solute dipole, reducing the magnitude of the reaction field E_{rxn} and the solvation energy, increasing the barrier height. On the other hand, saturation also reduces the screening ability of the solvent under applied field, enhancing E_{in} compared to its value calculated by neglecting dielectric saturation. These two effects are in competition when the applied field is in the positive direction, with the weakening of the reaction field being more dominant at low applied field strengths. Eventually, the applied field eliminates the screening ability of the solvent, leading to a recovery of electric field catalysis around $E_{\text{ext}} = 1.5$ V/nm.

Focusing on the case with $E_{\text{ext}} = 5$ V/nm, we find that the field reduces the barrier height by 1.0 kcal/mol when we neglect dielectric saturation but by 5.4 kcal/mol when we include it. This latter value is smaller than the lowering of 10.6 kcal/mol observed in simulations, but clearly a significant improvement, especially considering the simplicity of the model. Our Booth fit in Eq. (11) gives $\epsilon(E_{\text{ext}} = 5 \text{ V/nm}) = 4.2$, but MD simulations reported in Ref. 41 indi-

	ΔV^\ddagger	$\Delta G^\ddagger(0 \text{ V/nm})$	$\Delta G^\ddagger(5 \text{ V/nm})$	$\Delta\Delta G^\ddagger$
Present theory	25.5	17.3		
- Linear dielectric			16.3	-1.0
- Nonlinear dielectric			11.9	-5.4
- With electrofreezing			8.7	-8.6
Simulation [23]	27.4	18.9	8.3	-10.6

TABLE I. Comparison of the gas phase barrier ΔV^\ddagger and solution phase barrier ΔG^\ddagger , without and with an applied electric field, between the present theory and the atomistic simulation results of Ref. 23 for the Menshutkin reaction in acetonitrile solvent. The change to the solution phase barrier due to the electric field is denoted $\Delta\Delta G^\ddagger \equiv \Delta G^\ddagger(E) - \Delta G^\ddagger(0)$. Theoretical predictions are presented for the nonlinear theory that includes dielectric saturation, and the predictions of the linear theory are given in parentheses. All energies are in kcal/mol.

cated $\epsilon(E_{\text{ext}} = 5 \text{ V/nm}) \approx 2.4$, which when used in our theory predicts a barrier height reduction of 8.6 kcal/mol, in much better agreement with the results of Shaik and co-workers.²³ However, as pointed out in Ref. 41, this lower dielectric constant is due to an electrofreezing transition in acetonitrile that occurs around $E_{\text{ext}} \approx 3 \text{ V/nm}$ at room temperature. This important effect must be kept in mind when considering the application of strong electric fields to the catalysis of reactions in polar solvents.

Next, we apply the theory to the symmetric S_N2 reaction of F^- with CH_3F . The results are shown in Fig. 3. Using the same computational methods, we calculate a reaction barrier of $\Delta V^\ddagger = 8.6 \text{ kcal/mol}$ and dipole moments of $\mu_R = -5.8 \text{ D}$, $\mu_{\text{TS}} = 0$, such that $\mu_{\text{TS}}^2 - \mu_R^2 < 0$ and a polar solvent inhibits the reaction. For example, estimating $a = 0.3 \text{ nm}$ we find that the barrier height increases by 17.3 kcal/mol in acetonitrile.

Without accounting for dielectric saturation, an applied electric field is strongly screened by the polar solvent, as was observed for the Menshutkin reaction. However, significant differences emerge when we include dielectric saturation. Because the solvent reaction field leads to an increase in the barrier height, we find that the field-induced inhibition of solvation of the molecular dipole leads to a catalytic effect at low applied field strengths independent of the direction of the field. To the best of our knowledge, this effect—inhibition of reactant stabilization—is a new mode for electric field catalysis, and it would be simple to implement due to its independence of the field direction. For stronger fields, we see that the catalytic effect continues to grow when the field is positive, but reverses its behavior when the field is negative, because the external field and reaction field are now in competition.

This completes our development of an adiabatic TST of electric field catalysis with nonlinear dielectric effects. However, it is known that the dynamics of polar solvents can significantly impact the rate of reactions, especially those whose charge density changes significantly when crossing the barrier. In the next section, we consider these dynamical corrections using Grote-Hynes theory in the presence of an external electric field.

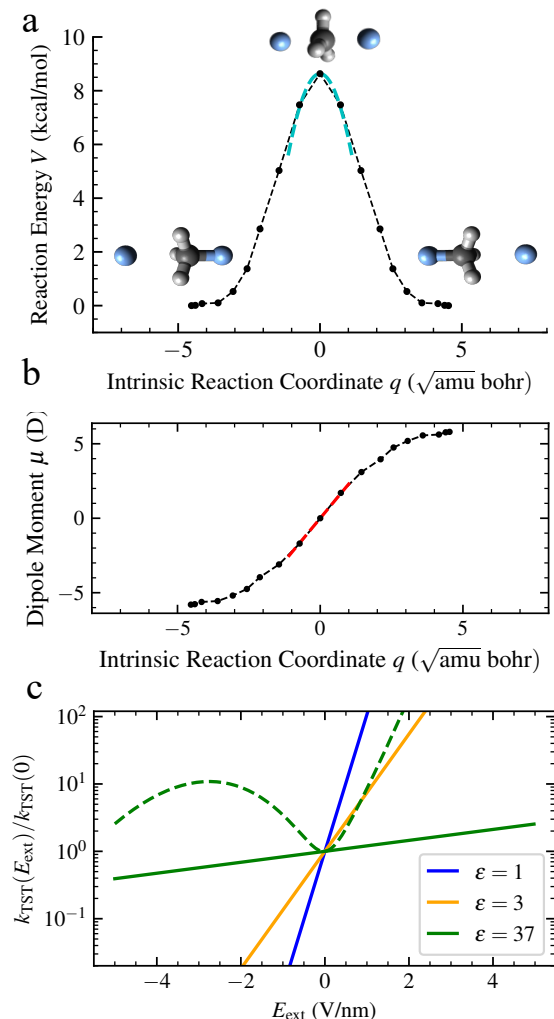


FIG. 3. Same as Fig. 2 but for the symmetric S_N2 reaction between CH_3F and F^- .

B. Dynamical Corrections

Within TST, the reaction is assumed to be adiabatic, i.e., the solvent responds instantaneously to changes in the molecular reaction dynamics. In reality, the solvent response lags, and recrossing events are responsible for a reduction in the rate constant compared to its TST value. Here, we incorporate dynamical corrections to the rate constant,

$$k_{\text{GH}} = \kappa k_{\text{TST}}, \quad (13)$$

where κ is the transmission factor calculated with Grote-Hynes theory.²⁸ We aim to understand how κ depends on the solvent polarity and the external electric field.

Specifically, we consider the dynamics of the IRC q near the TS, which we take to occur at $q = 0$. In this region, we treat the energy barrier as parabolic, and we linearize the transition state dipole moment $\mu_{\text{TS}}(q) \approx \mu'q$, as shown in Figs. 2 and 3, leading to the free energy surface⁴²

$$\begin{aligned} \Delta G(q) &= \Delta V^\ddagger - \frac{1}{2}\omega_{b,0}^2 q^2 - \frac{2|\mu'|^2}{a^3} \frac{\epsilon - 1}{2\epsilon + 1} q^2 \\ &\quad - \frac{3}{2\epsilon + 1} \mu' \cdot E_{\text{ext}} q \\ &\equiv \Delta V^\ddagger - \frac{1}{2}\omega_{b,\text{eq}}^2 q^2 - F_{\text{ext}} q, \end{aligned} \quad (14)$$

where $\omega_{b,0}$ is the barrier frequency in the gas phase, $\omega_{b,\text{eq}} = \sqrt{\omega_{b,0}^2 + 2\Lambda}$ is the (adiabatic) free energy barrier frequency, and

$$\Lambda = \frac{2|\mu'|^2}{a^3} \frac{\epsilon - 1}{2\epsilon + 1} \quad (15)$$

is the solvent reorganization energy (see below). In this limit, the dynamics is described by the generalized Langevin equation

$$\ddot{q} = -\omega_{b,\text{eq}}^2 q - \int_0^t dt' \zeta(t-t') \dot{q}(t') + \delta F_q(t) + F_{\text{ext}}, \quad (16)$$

where $\zeta(t)$ is a friction kernel due the interaction between the molecular dipole and the solvent, and $\delta F_q(t)$ is a random force satisfying the fluctuation-dissipation relation $\beta \langle \delta F_q(t) \delta F_q(0) \rangle = \zeta(t)$. The Grote-Hynes correction is

$$\kappa = \frac{\lambda^\ddagger}{\omega_{b,\text{eq}}}, \quad \lambda^\ddagger = \frac{\omega_{b,\text{eq}}^2}{\lambda^\ddagger + \hat{\zeta}(\lambda^\ddagger)}, \quad (17)$$

where the reactive frequency λ^\ddagger is the lowest positive root of the transcendental equation on the right.

As a model of the solvent dynamics, we use the Debye approximation to the dielectric function,⁴³⁻⁴⁶

$$\hat{\epsilon}(z) = 1 + \frac{\epsilon - 1}{1 + z\tau_D}, \quad (18)$$

where ϵ is the static dielectric constant, τ_D is the Debye relaxation time, and $\hat{f}(z)$ indicates the Laplace transform. Then, as shown in the Supporting Information, the friction kernel is given simply by

$$\hat{\zeta}(z) = \frac{\Lambda}{z + \tau_L^{-1}}, \quad (19)$$

where Λ is the reorganization energy in Eq. (15), and $\tau_L = 3\tau_D/(2\epsilon + 1)$ is the longitudinal relaxation time. In the time domain, this model yields simple exponential decay of the friction kernel, $\zeta(t) = \Lambda e^{-t/\tau_L}$.

Within a linear dielectric theory, a static external electric field does not modify the dynamics of equilibrium solvent fluctuations, and therefore the GH transmission coefficient is independent of the external field. However, if we allow the static dielectric constant (which enters the Debye model) to be field dependent owing to dielectric saturation, then the equilibrium solvent dynamics also acquire a field dependence.

We only present results for the symmetric S_N2 reaction, which we found to exhibit the largest dynamical corrections,

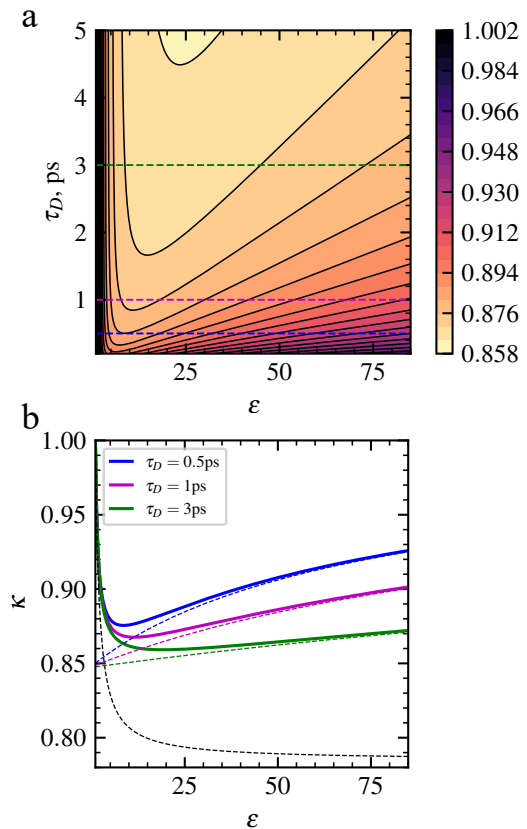


FIG. 4. Panel (a) shows the Grote-Hynes transmission coefficient κ as a function of the solvent's Debye relaxation time τ_D and static dielectric constant ϵ . The blue, magenta and green lines (bottom to top) are slices at $\tau_D = 0.5, 1,$ and 3 ps, results for which are shown in panel (b). For acetonitrile, $\tau_D \approx 3$ ps at room temperature. Also shown are the transmission coefficients obtained by artificially keeping τ_L constant (black dashed line) and Λ constant (colored dashed lines).

mostly due to its smaller cavity radius a (analogous results for the Menshutkin reaction are presented in the Supporting Information). For both reactions, we always find $\kappa > 0.8$, indicating that TST is a good approximation. From the IRC calculations of the S_N2 reaction, we extract $\mu' = 0.021$ D Bohr⁻¹ amu^{-0.5} and $\omega_{b,0} = 450.4$ cm⁻¹.

In Fig. 4, we plot the Grote-Hynes transmission coefficient κ as a function of the Debye relaxation time τ_D and static dielectric constant ϵ . Interestingly, for fixed τ_D , we see non-monotonic behavior as a function of ϵ . Results at three example values of $\tau_D = 0.5, 1,$ and 3 ps are shown in panel (b), where $\tau_D \approx 3$ ps is representative of acetonitrile at room temperature.⁴⁷ Such non-monotonic behavior is usually associated with a resonance between the solvent response function and the barrier frequency.⁴⁸ However, as we show in Fig. 4(b), the minimum in κ occurs at a much lower frequency than that of the reaction barrier.

The non-monotonic behavior arises instead because both the reorganization energy Λ and the longitudinal relaxation time τ_L depend on ϵ , with opposite effects on the transmission coefficient. With increasing ϵ , the reorganization energy increases

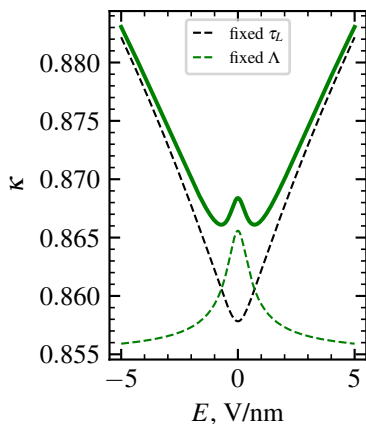


FIG. 5. The effect of dielectric saturation (nonlinearities) on the Grote-Hynes correction κ for the symmetric S_N2 reaction in acetonitrile. As in Fig. 4, we also show results obtained when τ_L and Λ are separately held constant.

from 0 to $|\mu'|^2/a^3$, reflecting stronger coupling between the dipole and the solvent, which increases the probability of re-crossing and thus lowers κ . However, with increasing ϵ , the longitudinal relaxation time τ_L decreases from $3\tau_D$ to 0, reflecting a more adiabatic solvent response, which increases κ . It is the competition of these two effects that yields the non-monotonic behavior. To observe the two effects in isolation, we also show results obtained by artificially keeping τ_L constant (dashed black line), and Λ constant (colored dashed lines) in Fig. 4.

Finally, we consider the effect of dielectric saturation on solvent dynamics. As mentioned before, the Grote-Hynes transmission coefficient only depends on the applied electric field through the modified dielectric constant. In Fig. 5, we plot transmission coefficients obtained for different applied field strengths, specifically for the case of acetonitrile with zero-field values $\epsilon = 37$ and $\tau_D = 3$ ps (we assume that τ_D is unaffected by the applied field strength, but this assumption would have to be tested). With increasing field, ϵ is reduced and, since κ shows a nonmonotonic dependence on ϵ , a similar variation is also observed with applied field strength. As in Fig. 4, the two competing effects responsible for this nonmonotonic dependence arise from the simultaneous modulation of the longitudinal relaxation time τ_L and the reorganization energy Λ .

III. CONCLUSIONS

We have developed a theory for reaction rates in polar solvents in the presence of an externally applied electric field parameterized by only a few physical values. Importantly, we accounted for dielectric saturation, i.e., the reduction of the solvent dielectric constant in the presence of an external electric field. In the TST approximation, we used our theory to study the Menshutkin methyl transfer reaction between CH_3I and pyridine and the S_N2 reaction between CH_3F and

F^- . Despite its simplicity, we find that our theory is in nearly quantitative agreement with results obtained using fully atomistic simulations.²³ We therefore expect that our theory will be useful to experimentalists and others interested in rapid predictions without the cost of atomistic simulations. Our results confirm the recovery of electric field catalysis at large field strengths due to dielectric saturation, but we warn about the possibility of electrofreezing of the solvent.

Finally, we relax the adiabatic approximation by computing Grote-Hynes dynamical corrections to the rate constant within the Debye model for the solvent. We considered dynamical corrections to TST via Grote-Hynes theory, but for the two reactions studied, we find that dynamical corrections reduce the TST rate by only about 20%. We observe an interesting non-monotonic dependence of the correction factor on the electric field strength, due to the opposite ways in which the solvent reorganization energy and longitudinal relaxation time depend on the field through the dielectric constant. However, the scale of the variations in the correction factor is only about 2% over an accessible range of electric field strengths.

Despite the successes of our theory, it has several limitations. We have neglected polarizability and higher order responses, and we have described the solvent using simple dielectric continuum theory. Although we employed simple models for the dielectric constant's saturating behavior and dynamical response, these can be easily replaced by more accurate parameterizations or experimental data. Finally, we have ignored the rotational dynamics of the reacting complex. It would be useful to understand the impact of all of these approximations in cases where our theory fails to agree with experiment.

ACKNOWLEDGEMENTS

T.C.B. thanks David Limmer and Latha Venkataraman for helpful discussions. This work was supported by the Columbia Center for Computational Electrochemistry. We acknowledge computing resources from Columbia University's Shared Research Computing Facility project, which is supported by NIH Research Facility Improvement Grant 1G20RR030893-01, and associated funds from the New York State Empire State Development, Division of Science Technology and Innovation (NYSTAR) Contract C090171, both awarded April 15, 2010.

IV. REFERENCES

1. S. Shaik, D. Mandal, and R. Ramanan, "Oriented electric fields as future smart reagents in chemistry," *Nat. Chem.* **8**, 1091–1098 (2016).
2. S. Ciampi, N. Darwish, H. M. Aitken, I. Díez-Pérez, and M. L. Coote, "Harnessing electrostatic catalysis in single molecule, electrochemical and chemical systems: a rapidly growing experimental tool box," *Chem. Soc. Rev.* **47**, 5146–5164 (2018).
3. S. Shaik, R. Ramanan, D. Danovich, and D. Mandal, "Structure and reactivity/selectivity control by oriented-external electric fields," *Chem. Soc. Rev.* **47**, 5125–5145 (2018).

- ⁴T. Stuyver, D. Danovich, J. Joy, and S. Shaik, "External electric field effects on chemical structure and reactivity," *WIREs Comput. Mol. Sci.* **10** (2019), 10.1002/wcms.1438.
- ⁵V. V. Welborn, L. Ruiz Pestana, and T. Head-Gordon, "Computational optimization of electric fields for better catalysis design," *Nature Catalysis* **1**, 649–655 (2018).
- ⁶A. C. Aragonès, N. L. Haworth, N. Darwish, S. Ciampi, N. J. Bloomfield, G. G. Wallace, I. Diez-Perez, and M. L. Coote, "Electrostatic catalysis of a diels–alder reaction," *Nature* **531**, 88–91 (2016).
- ⁷Y. Zang, Q. Zou, T. Fu, F. Ng, B. Fowler, J. Yang, H. Li, M. L. Steigerwald, C. Nuckolls, and L. Venkataraman, "Directing isomerization reactions of cumulenes with electric fields," *Nat. Commun.* **10** (2019), 10.1038/s41467-019-12487-w.
- ⁸C. F. Gorin, E. S. Beh, Q. M. Bui, G. R. Dick, and M. W. Kanan, "Interfacial electric field effects on a carbene reaction catalyzed by rh porphyrins," *J. Am. Chem. Soc.* **135**, 11257–11265 (2013).
- ⁹L. Zhang, E. Laborda, N. Darwish, B. B. Noble, J. H. Tyrell, S. Pluczyk, A. P. Le Brun, G. G. Wallace, J. Gonzalez, M. L. Coote, and S. Ciampi, "Electrochemical and electrostatic cleavage of alkoxyamines," *J. Am. Chem. Soc.* **140**, 766–774 (2018).
- ¹⁰M. Klinska, L. M. Smith, G. Gryn'ova, M. G. Banwell, and M. L. Coote, "Experimental demonstration of ph-dependent electrostatic catalysis of radical reactions," *Chem. Sci.* **6**, 5623–5627 (2015).
- ¹¹M. T. Blyth and M. L. Coote, "A ph-switchable electrostatic catalyst for the diels–alder reaction: Progress toward synthetically viable electrostatic catalysis," *J. Org. Chem.* **84**, 1517–1522 (2019).
- ¹²M. Shetty, M. A. Ardagh, Y. Pang, O. A. Abdelrahman, and P. J. Dauenhauer, "Electric-field-assisted modulation of surface thermochemistry," *ACS Catalysis* **10**, 12867–12880 (2020).
- ¹³S. Shaik, D. Danovich, J. Joy, Z. Wang, and T. Stuyver, "Electric-field mediated chemistry: Uncovering and exploiting the potential of (oriented) electric fields to exert chemical catalysis and reaction control," *J. Am. Chem. Soc.* **142**, 12551–12562 (2020).
- ¹⁴M. Calvaresi, R. V. Martinez, N. S. Losilla, J. Martinez, R. Garcia, and F. Zerbetto, "Splitting co₂ with electric fields: A computational investigation," *The Journal of Physical Chemistry Letters* **1**, 3256–3260 (2010).
- ¹⁵P. Besalú-Sala, M. Solà, J. M. Luis, and M. Torrent-Sucarrat, "Fast and simple evaluation of the catalysis and selectivity induced by external electric fields," *ACS Catalysis* **11**, 14467–14479 (2021).
- ¹⁶L. Rincón, J. R. Mora, F. J. Torres, and R. Almeida, "On the activation of σ -bonds by electric fields: A valence bond perspective," *Chemical Physics* **477**, 1–7 (2016).
- ¹⁷N. M. Hoffmann, X. Wang, and T. C. Berkelbach, "Linear free energy relationships in electrostatic catalysis," *ACS Catal.* **12**, 8237 (2022).
- ¹⁸K. Gopakumar, S. Shaik, and R. Ramanan, "Two-way catalysis in a diels–alder reaction limits inhibition induced by an external electric field," *Angewandte Chemie* **135** (2023), 10.1002/ange.202307579.
- ¹⁹W. Lai, H. Chen, K.-B. Cho, and S. Shaik, "External electric field can control the catalytic cycle of cytochrome p450cam: A qm/mm study," *The Journal of Physical Chemistry Letters* **1**, 2082–2087 (2010).
- ²⁰M. R. Talipov and Q. K. Timerghazin, "Protein control of s-nitrosothiol reactivity: Interplay of antagonistic resonance structures," *The Journal of Physical Chemistry B* **117**, 1827–1837 (2013).
- ²¹S. Yan, X. Ji, W. Peng, and B. Wang, "Evaluating the transition state stabilization/destabilization effects of the electric fields from scaffold residues by a qm/mm approach," *The Journal of Physical Chemistry B* **127**, 4245–4253 (2023).
- ²²V. Vaissier, S. C. Sharma, K. Schaettle, T. Zhang, and T. Head-Gordon, "Computational optimization of electric fields for improving catalysis of a designed kemp eliminase," *ACS Catalysis* **8**, 219–227 (2017).
- ²³K. Dutta Dubey, T. Stuyver, S. Kalita, and S. Shaik, "Solvent organization and rate regulation of a menshutkin reaction by oriented external electric fields are revealed by combined md and qm/mm calculations," *J. Am. Chem. Soc.* **142**, 9955 (2020).
- ²⁴Z. Jiang, P. P. Bazianos, Z. Yan, and A. M. Rappe, "Mechanism of water dissociation with an electric field and a graphene oxide catalyst in a bipolar membrane," *ACS Catalysis* **13**, 7079–7086 (2023).
- ²⁵L. Wang, S. D. Fried, and T. E. Markland, "Proton network flexibility enables robustness and large electric fields in the ketosteroid isomerase active site," *The Journal of Physical Chemistry B* **121**, 9807–9815 (2017).
- ²⁶G. Cassone, J. Sponer, and F. Saija, "Ab initio molecular dynamics studies of the electric-field-induced catalytic effects on liquids," *Topics in Catalysis* **65**, 40–58 (2021).
- ²⁷H. Eyring, "The activated complex in chemical reactions," *J. Chem. Phys.* **3**, 107 (1935).
- ²⁸R. F. Grote and J. T. Hynes, "The stable states picture of chemical reactions. ii. rate constants for condensed and gas phase reaction models," *J. Chem. Phys.* **73**, 2715 (1980).
- ²⁹L. Onsager, "Electric moments of molecules in liquids," *J. Am. Chem. Soc.* **58**, 1486 (1936).
- ³⁰F. Booth, "The dielectric constant of water and the saturation effect," *J. Chem. Phys.* **19**, 391 (1951).
- ³¹M. Sola, A. Lledos, M. Duran, J. Bertran, and J. L. M. Abboud, "Analysis of solvent effects on the menshutkin reaction," *J. Am. Chem. Soc.* **113**, 2873–2879 (1991).
- ³²H. Castejon and K. B. Wiberg, "Solvent effects on methyl transfer reactions. 1. the menshutkin reaction," *J. Am. Chem. Soc.* **121**, 2139–2146 (1999).
- ³³F. Neese, "Software update: the orca program system, version 4.0," *WIREs Comput. Mol. Sci.* **8**, e1327 (2017).
- ³⁴K. Fukui, S. Kato, and H. Fujimoto, "Constituent analysis of the potential gradient along a reaction coordinate. method and an application to methane + tritium reaction," *J. Am. Chem. Soc.* **97**, 1 (1975).
- ³⁵K. Ishida, K. Morokuma, and A. Komornicki, "The intrinsic reaction coordinate. an ab initio calculation for HNC \rightarrow HCN and H⁻+CH₄ \rightarrow CH₄+H⁻," *J. Chem. Phys.* **66**, 2153 (1977).
- ³⁶A. D. Becke, "Density-functional exchange-energy approximation with correct asymptotic behavior," *Phys. Rev. A* **38**, 3098 (1988).
- ³⁷A. D. Becke, "A new mixing of hartree–fock and local density-functional theories," *J. Chem. Phys.* **98**, 1372 (1993).
- ³⁸A. Schäfer, C. Huber, and R. Ahlrichs, "Fully optimized contracted gaussian basis sets of triple zeta valence quality for atoms li to kr," *J. Chem. Phys.* **100**, 5829 (1994).
- ³⁹F. Weigend and R. Ahlrichs, "Balanced basis sets of split valence, triple zeta valence and quadruple zeta valence quality for h to rn: Design and assessment of accuracy," *Phys. Chem. Chem. Phys.* **7**, 3297 (2005).
- ⁴⁰H. T. Turan, S. Brickel, and M. Meuwly, "Solvent effects on the menshutkin reaction," *J. Phys. Chem. B* **126**, 1951 (2022).
- ⁴¹I. N. Daniels, Z. Wang, and B. B. Laird, "Dielectric properties of organic solvents in an electric field," *J. Phys. Chem. C* **121**, 1025 (2017).
- ⁴²G. R. Haynes and G. A. Voth, "The dependence of the potential of mean force on the solvent friction: Consequences for condensed phase activated rate theories," *J. Chem. Phys.* **99**, 8005 (1993).
- ⁴³T.-W. Nee and R. Zwanzig, "Theory of dielectric relaxation in polar liquids," *J. Chem. Phys.* **52**, 6353 (1970).
- ⁴⁴B. Bagchi, D. W. Oxtoby, and G. R. Fleming, "Theory of the time development of the stokes shift in polar media," *Chem. Phys.* **86**, 257 (1984).
- ⁴⁵G. Van der Zwan and J. T. Hynes, "Time-dependent fluorescence solvent shifts, dielectric friction, and nonequilibrium solvation in polar solvents," *The Journal of Physical Chemistry* **89**, 4181 (1985).
- ⁴⁶G. Moro, P. Nordio, and A. Polimeno, "Multivariate diffusion models of dielectric friction and tict transitions," *Mol. Phys.* **68**, 1131 (1989).
- ⁴⁷A. Stoppa, A. Nazet, R. Buchner, A. Thoman, and M. Walther, "Dielectric response and collective dynamics of acetonitrile," *J. Mol. Liq.* **212**, 963 (2015).
- ⁴⁸X. Li, A. Mandal, and P. Huo, "Cavity frequency-dependent theory for vibrational polariton chemistry," *Nat. Commun.* **12**, 1315 (2021).

Supporting Information for: Reaction Rate Theory for Electric Field Catalysis in Solution

S1. COMPUTATIONAL DETAILS

All unrestricted density functional theory (DFT) calculations were performed with the ORCA quantum chemistry package³³ using the B3LYP functional³⁶ and the def2-TZVP^{38,39} basis set. For both reactions, the transition state (TS) geometry was first optimized starting with a reasonable guess structure. Next, an intrinsic reaction coordinate^{34,35} (IRC) calculation was performed using the optimized TS to obtain the reaction energy profile. The IRCs were converged with a maximum gradient threshold of 1×10^{-3} Hartree/Bohr and a root-mean-square gradient threshold of 2×10^{-4} Hartree/Bohr. Finally, for each geometry obtained from the IRC calculation, a separate single point calculation was performed at the same level of theory to extract the dipole moment.

S2. DERIVATION OF THE FRICTION KERNEL

Here we derive the GLE friction kernel relevant for the interaction between a continuum polar solvent and a dipole whose magnitude can change with time. The friction kernel $\zeta(t)$ is related to the fluctuating random force $\delta F_q(t)$ by the fluctuation-dissipation relation

$$\zeta(t) = \beta \langle \delta F_q(t) \delta F_q(0) \rangle = \frac{|\mu'|^2}{3k_B T} \langle \mathbf{E}_{\text{rxn}}(t) \cdot \mathbf{E}_{\text{rxn}}(0) \rangle \quad (\text{S1})$$

where $\langle \mathbf{E}_{\text{rxn}}(t) \cdot \mathbf{E}_{\text{rxn}}(0) \rangle$ is the equilibrium correlation function of the fluctuations of the reaction field. The dynamics of the reaction field follow those of the dipole moment via

$$\mathbf{E}_{\text{rxn}}(t) = \int_{-\infty}^t dt' \chi(t-t') \boldsymbol{\mu}(t'). \quad (\text{S2})$$

where the response function is

$$\chi(t) = -\frac{\beta}{3} \frac{d}{dt} \langle \mathbf{E}_{\text{rxn}}(t) \cdot \mathbf{E}_{\text{rxn}}(0) \rangle \quad (\text{S3})$$

Combining Eqs. (S1) and (S3) relates the friction kernel to the response function,

$$\frac{d\zeta(t)}{dt} = -|\mu'|^2 \chi(t) \quad \text{or} \quad z \hat{\zeta}(z) - \Lambda = -|\mu'|^2 \hat{\chi}(z), \quad (\text{S4})$$

where we have taken the Laplace transform, and $\Lambda \equiv \zeta(t=0)$ is the reorganization energy. Within our model of a dipole in a spherical cavity, a boundary value problem yields the response function

$$\hat{\chi}(z) = \frac{2}{a^3} \frac{\hat{\epsilon}(z) - 1}{2\hat{\epsilon}(z) + 1}. \quad (\text{S5})$$

Using the Debye approximation for the dielectric function presented in the text gives the friction kernel

$$\hat{\zeta}(z) = \frac{\Lambda}{z + \tau_L^{-1}} \quad \text{or} \quad \zeta(t) = \Lambda e^{-t/\tau_L}, \quad \text{with} \quad \Lambda = \frac{2|\mu'|^2}{a^3} \frac{\epsilon - 1}{2\epsilon + 1}. \quad (\text{S6})$$

S3. DYNAMICAL CORRECTION FACTOR FOR THE MENSCHUTKIN REACTION

Since the Grote-Hynes correction to the transition state theory (TST) rate constant was found to be qualitatively identical for the two reactions, only results for the S_N2 reaction were shown in the main text. We provide the analogous figures for the Menshutkin reaction in Fig. S1, for comparison.

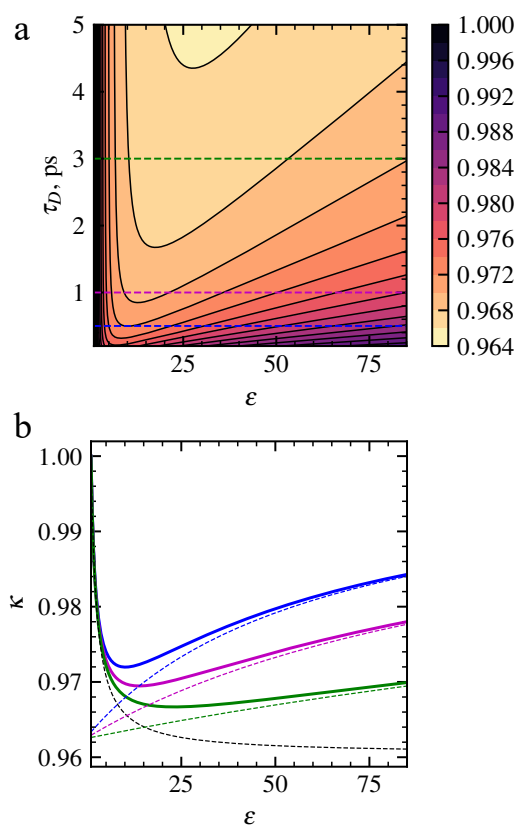


FIG. S1. The Grotte-Hynes transmission coefficient κ as a function of the solvent's Debye relaxation time τ_D and static dielectric constant ϵ for the Menshutkin reaction (panel (a)). The blue, magenta and green lines (bottom to top) are slices at $\tau_D = 0.5, 1,$ and 3 ps, results for which are shown in panel (b).